SLAC-PUB-11613
January 2006

**2005 ALCPG & ILC Workshops - Snowmass, U.S.A.**

# Optics of the ILC Extraction Line for 2 mrad Crossing Angle

Y. Nosochkov, K. Moffeit, A. Seryi, C. Spencer, M. Woods
*Stanford Linear Accelerator Center, Menlo Park, CA 94025, USA*
D. Angal-Kalinin, R. Appleby
*ASTeC, Daresbury Laboratory, Warrington, WA4 4AD, England*
B. Parker
*Brookhaven National Laboratory, Upton, NY 11973, USA*

The ILC extraction line for 2 mrad crossing angle is under development by the SLAC-BNL-UK-France task force collaboration. This report describes the progress in the 2 mrad optics design which includes the changes to the final focus doublet, the complete optics for the extraction diagnostics, and the changes to the sextupole and collimation systems. The results of disrupted beam tracking simulations are presented.

## 1. INTRODUCTION

The main requirements for the ILC extraction line are to transport the high power primary $e^+/e^-$ beam and the beamstrahlung (BS) photons to dumps with a tolerable beam loss on magnets and acceptable detector background, and to provide a proper optics for the post collision beam diagnostics. Two designs of the ILC extraction line are being developed, for 2 mrad and 20 mrad crossing angles [1]-[4]. The advantage of the smaller crossing angle is a lower geometric luminosity loss and therefore less dependence on a crab cavity correction. The smaller angle also reduces bending and synchrotron radiation (SR) in the detector solenoid, and lowers the detector background [5]. However, due to the small beam separation after the interaction point (IP), the incoming and extraction beams must share the final focus (FF) magnets which complicates the 2 mrad extraction optics and the magnet design. Below, we present the current 2 mrad optics and the results of disrupted beam tracking simulations.

## 2. EXTRACTION OPTICS

The presented below 2 mrad extraction optics is an upgrade of the earlier version described in [1, 2]. Fig. 1 shows the top view of the 2 mrad crossing on one side of the IP. The incoming beam is on-center in the shared QD0, SD0, QF1 and SF1 magnets, and the extraction beam and BS photons are horizontally offset and at an angle in these magnets. The distance from the IP to the first quadrupole QD0 is 4.5 m. In this scheme, the QD0, SD0 and SF1 are the large bore superconducting (SC) magnets with the aperture radius of R = 35 mm, 88 mm and 112 mm, respectively, accommodating both the primary beams and the BS photons. It is proposed that the design of the QD0 would be based on NbTi technology for the baseline 0.5 TeV center of mass energy (CM) and then upgraded to a more advanced but difficult Nb3Sn design for 1 TeV CM [6]. The QF1 is a conventional iron quadrupole with a small 10 mm aperture for the incoming beam. The extraction beam is horizontally offset by about 60 mm in the QF1 and passes through the aperture of its coil pocket. The non-linear field in the QF1 coil pocket is modeled as a multipole field for extraction optics calculations.

There are several complications arising from the small crossing angle. The focusing in the shared FF magnets is constrained by the incoming optics, therefore it can be only partially optimized for the extraction beam. The beam offset in the shared magnets creates dispersion which has a non-linear effect due to a long low energy tail in the disrupted beam. The shared SD0 and SF1 sextupoles create the non-linear geometric aberrations increasing the



Work supported in part by Department of Energy contract DE-AC02-76SF00515

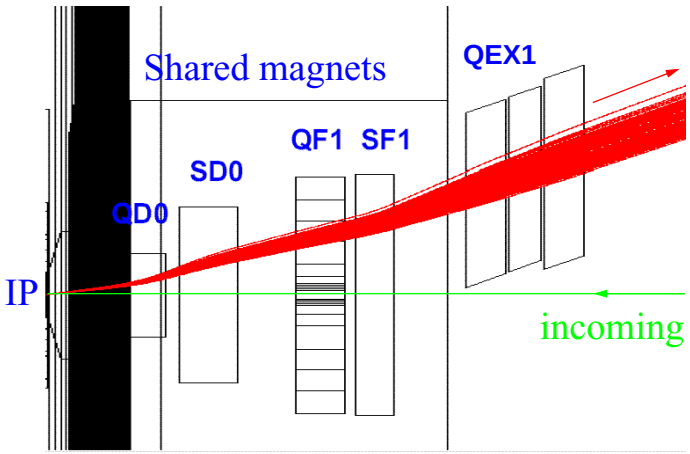


Figure 1: Top view of the 2 mrad crossing on one side of the IP showing the incoming (green) and extraction (red) beams.

beam size. The small beam separation requires a special design of the extraction magnet just after the FF magnets. The extraction electron and BS photon beams diverge in the shared magnets and require separate lines and dumps.

Although the FF shared magnets are constrained by the incoming optics, it was possible to optimize the magnet field, length, aperture and position to improve the focusing of the extraction beam. In particular, the magnet parameters were adjusted to minimize the low energy overfocusing and the beam loss on the sensitive SC magnets. The disrupted beam can be either at a positive or a negative 2 mrad angle with respect to the incoming beam, however the optimization showed that only one sign of the angle is acceptable for the disrupted beam focusing. This is because the shared FF sextupoles would create either the horizontal focusing or defocusing depending on the sign of the disrupted beam offset. The selected optimum sign of the 2 mrad angle provides the horizontal focusing in the SD0 sextupole which reduces the initial defocusing and chromatic dispersion created in the QD0.

The first independent extraction quadrupole QEX1A starts at about 35 m after the IP. The complications are that it has a large 113 mm aperture, but the beams are separated only by 150 mm, and the magnet fringe field on the incoming line must be low. Currently, two designs have been suggested. The SC super septum quadrupole design [7] would provide the large aperture for the extraction beam and BS photons and a hole in the iron for the incoming beam. The second proposal is to use a Panofsky style water cooled septum magnet [8].

The beta functions and linear dispersion in the complete extraction line are shown in Fig. 2. The optics includes three vertical chicanes with the peak vertical dispersion of 6.9 cm, 6.9 cm and 2 cm, respectively. The first chicane is used for collimation of the disrupted low energy tail, and the next two chicanes are included for energy and polarization diagnostics [9, 10]. Additionally, the optics provides the 2nd focus at the center of the polarization chicane to obtain the required $<$100 $\mu$m beam size. The angular transformation term $R_{22}$ from the IP to the 2nd focus is adjusted to -0.5, one of the optimum values for the polarization measurement.

The extraction line also includes the horizontal bends which have two functions. First, they create the necessary horizontal trajectory for the extraction beam. This includes the beam deflection for the specified $>$3.5 m separation between the electron dump and the incoming line, and the 2 mrad angle at the 2nd focus, same as at the IP, required for the polarization diagnostics. Secondly, the bends are adjusted to minimize the low energy orbits in order to reduce the beam loss. The horizontal dispersion at the 2nd focus is -7 cm which is acceptable for the diagnostics.

Most of the extraction beam loss is caused by overfocusing of the lowest energy particles in the disrupted beam energy tail. To minimize this loss, a large chromatic acceptance is required. This was achieved by optimizing the strengths and positions of the quadrupoles and bends, and using sufficiently large apertures. Further reduction of the chromatic effects could be achieved by including extraction sextupoles. However, the study showed that the 3rd order geometric aberrations from additional sextupoles would increase the beam size at the 2nd focus to unacceptable level for polarization measurement. For this reason, the new sextupoles were not included in this optics. Therefore, the

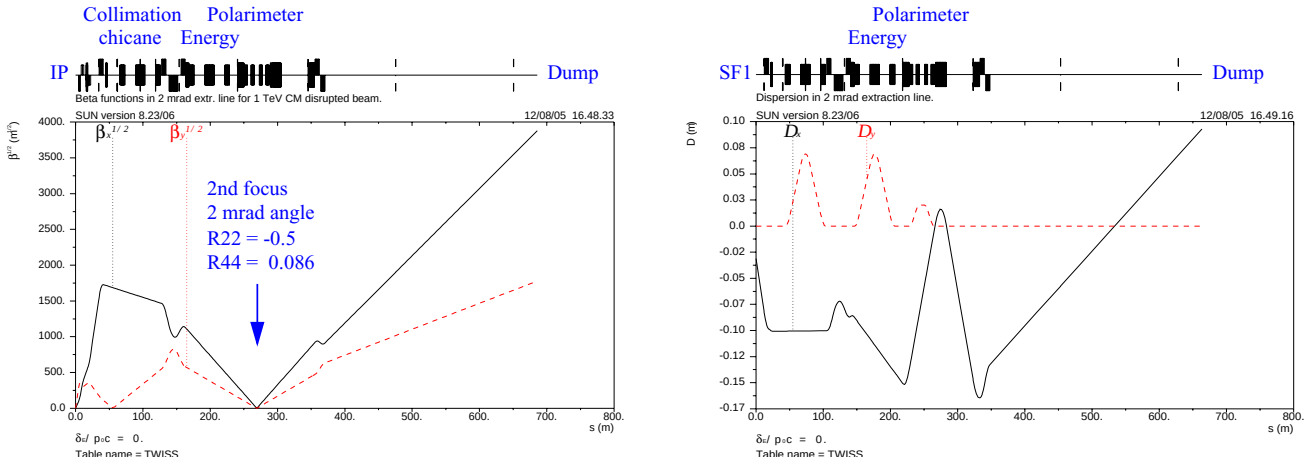


Figure 2: Beta functions (left) and linear dispersion (right) in the 2 mrad extraction line.

only sextupoles in the extraction line are the shared SD0 and SF1 magnets. Tracking of the disrupted beam with 1 TeV CM nominal parameters [11] showed that 15% of the beam charge is contained within 100×100 $\mu$m$^2$ size at the 2nd focus. Finally, the optics includes several protection collimators to further reduce the beam loss on extraction magnets. These collimators are positioned to collimate the low energy tail.

At the end of the beamline, the optics includes a long ∼315 m drift to the electron dump which provides the required >3.5 m horizontal separation between the dump and the incoming line. This drift includes two collimators to limit the disrupted beam size to 15 cm radius of the dump window [12]. The long drift also naturally increases the small size of the undisrupted beam helping to avoid damage to the dump window. However, a significantly larger size is required to prevent the water boiling in the dump vessel [12]. We consider that such an increase of the beam size can be achieved by using a rastering system in front of the dump for sweeping the bunches over a wide area on the dump window.

Since the BS photon beam is not bent in the magnets, it will diverge from the primary $e^+/e^-$ beam and after ∼50 m will require a separate line and a dump. The size of the photon aperture is limited by the small separation with the incoming line. The proposed aperture would accept the photons with up to ±0.5 mrad angles at the IP which is sufficient for the ILC nominal luminosity options [11]. It is proposed that the separate photon dump would be installed at about 350–400 m after the IP.

This optics is designed for up to 1 TeV CM energy. The parameters of the extraction magnets at 1 TeV CM are listed in Table I, where N, L, B, R and $\theta$ are the magnet number, magnet length, field, aperture radius, and bending angle, respectively.

## 3. PARTICLE TRACKING

In tracking simulations, the disrupted beam was transported from the IP to the dump using the TURTLE code [13]. The disrupted distribution at the IP was simulated for the 1 TeV CM nominal ILC parameters and included the realistic energy spread $\Delta E/E_0$ from 0 to -80% and the angular spread up to $X'_{max} = 496$ $\mu$rad and $Y'_{max} = 566$ $\mu$rad. These maximum angles correspond to the worst case scenario when there is a large vertical position offset $\Delta y$ between the beams at the IP which significantly increases the vertical divergence.

Fig. 3 shows the horizontal and vertical disrupted beam envelopes for various energy ranges from $\Delta E/E_0 = 0$ to -80% at 1 TeV CM. The horizontal bump at s ∼ 300 m corresponds to the polarization chicane where the horizontal angle is set to 2 mrad, as at the IP, required for diagnostics. The last two collimators reduce the disrupted beam size to 15 cm radius of the dump window. The BS photon beam horizontally diverges from the electrons and requires a

Table I: Quadrupole, bend and sextupole parameters at 1 TeV CM.

| Quadrupole | N | L (m) | B′ (T/m) | R (mm) |
|---|---|---|---|---|
| QD0 | 1 | 2.5 | -159.78 | 35 |
| QF1 | 1 | 2.0 | 67.93 | 10 |
| QEX1A | 1 | 3.0 | 11.76 | 113 |
| QEX1B | 1 | 3.0 | 10.46 | 127 |
| QEX3 | 2 | 3.0 | 6.83 | 150 |
| QEX4 | 4 | 3.0 | -7.42 | 150 |
| QEX5 | 2 | 3.0 | 6.83 | 150 |
| QEX6 | 2 | 3.0 | 5.77 | 150 |
| QEX7 | 2 | 3.0 | -5.59 | 150 |

| Bend | N | L (m) | B (T) | $\theta$ (mrad) |
|---|---|---|---|---|
| BHEX1 | 1 | 2.0 | 0.417 | 0.5 |
| BHEX2 | 2 | 2.0 | -0.598 | -0.717 |
| BHEX3 | 4 | 2.0 | 0.929 | 1.114 |
| BHEX4 | 7 | 2.0 | -0.867 | -1.040 |
| BHEX5 | 4 | 2.0 | 0.806 | 0.967 |
| BYCHIC | 6 | 2.0 | 0.834 | 1.0 |
| BYCHICM | 6 | 2.0 | -0.834 | -1.0 |
| BYENE | 6 | 2.0 | 0.834 | 1.0 |
| BYENEM | 6 | 2.0 | -0.834 | -1.0 |

| Bend | N | L (m) | B (T) | $\theta$ (mrad) |
|---|---|---|---|---|
| BYPOL | 4 | 2.0 | 0.834 | 1.0 |
| BYPOLM | 4 | 2.0 | -0.834 | -1.0 |

| Sextupole | N | L (m) | B″ (T/m$^2$) | R (mm) |
|---|---|---|---|---|
| SD0 | 1 | 3.8 | 1043.1 | 88 |
| SF1 | 1 | 3.8 | -340.1 | 112 |

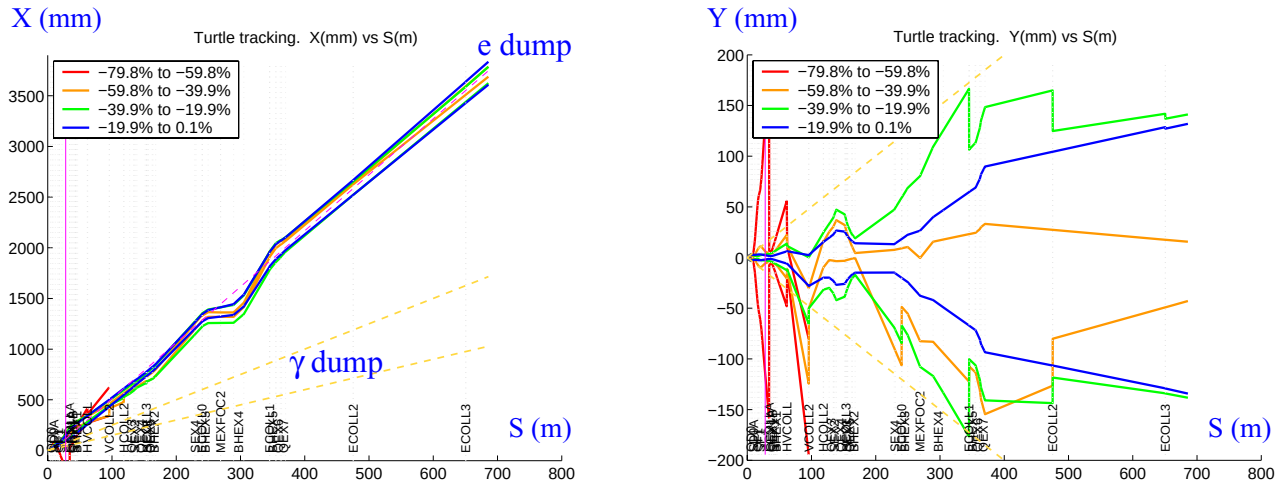


Figure 3: Horizontal (left) and vertical (right) electron and BS photon envelopes in the extraction line for various energy ranges from the IP to the dumps.

separate dump. The photon aperture is chosen to accept the photons with up to ±0.5 mrad angles at the IP which is sufficient for the ILC nominal luminosity options.

The detailed beam distributions in the first extraction magnets are shown in Fig. 4, where the incoming beam center is indicated by "+" and the photon aperture is shown by the yellow box. Notice that the extraction beam passes through the coil pocket in the conventional QF1 quadrupole. The cross section of the first separate extraction quadrupole QEX1A corresponds to the SC super septum design where the quadrupole has a 50 mm hole in the iron for the incoming beam.

Table II shows the power loss at individual elements for the collisions without offset and with $\Delta y = 100$ nm offset at the IP, where S is the distance after the IP. The power loss increases with the vertical IP offset due to the enlarged vertical divergence. However the large $\Delta y$ events will be rare, hence they should not significantly increase the average loss. The loss on the SC magnets at $\Delta y = 0$ is within several Watts which should be acceptable. Most of the loss is on the collimators labeled with "COLL" in the name. We conclude that the electron power loss in the 2 mrad extraction line is within the acceptable level for the ILC nominal parameters for up to 1 TeV CM energy. Further simulations for a high luminosity beam options showed that the loss on the SC magnets becomes unacceptable. More optimization of the 2 mrad design is needed to further reduce the beam loss.

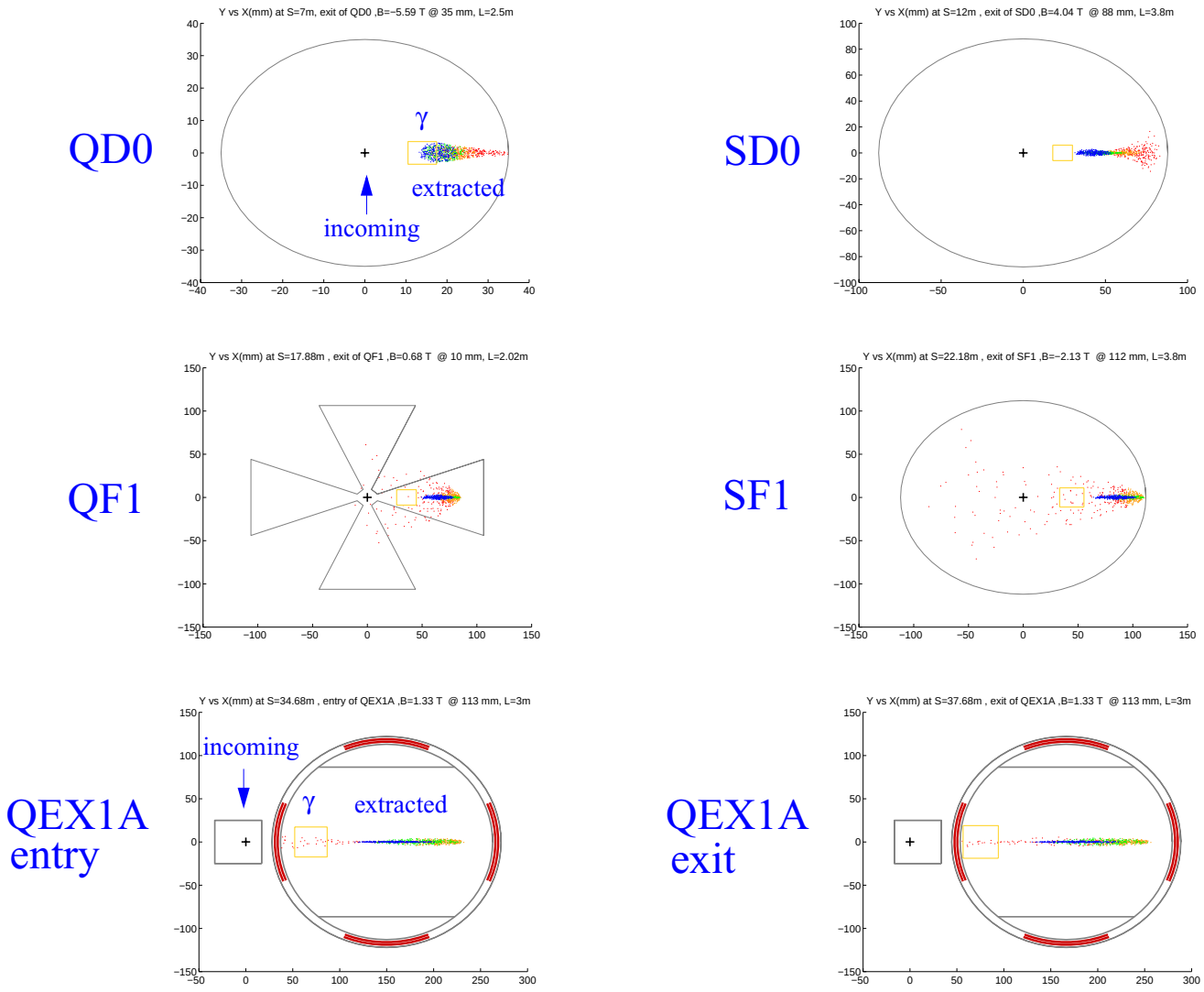


Figure 4: Disrupted beam distribution at magnet cross sections. The "+" shows the center of the incoming beam, and the yellow box is the aperture for ±0.5 mrad BS photon beam.

Table II: Disrupted beam loss at 1 TeV CM for collisions without offset and with $\Delta y = 100$ nm offset at the IP.

| Name | S (m) | P (kW) | |
|---|---|---|---|
| | | $\Delta y = 0$ | 100 nm |
| QD0 | 5.75 | 0.0003 | 0.001 |
| SD0 | 10.10 | 0 | 0.001 |
| QF1 | 18.03 | 0 | 0.044 |
| ECOLLA | 34.08 | 0.050 | 0.25 |
| QEX1A | 34.68 | 0.004 | 0.013 |
| HCOLL | 61.58 | 0.002 | 0.005 |
| VCOLL | 61.88 | 0.002 | 7.05 |
| BYCHIC | 89.18 | 0.024 | 0.049 |

| Name | S (m) | P (kW) | |
|---|---|---|---|
| | | $\Delta y = 0$ | 100 nm |
| BYCHIC | 91.48 | 0.003 | 0.006 |
| BYCHIC | 93.78 | 0.003 | 0.004 |
| VCOLL2 | 95.78 | 44.3 | 65.9 |
| HCOLL2 | 118.48 | 8.06 | 55.2 |
| HCOLL3 | 153.58 | 8.41 | 23.5 |
| ECOLL0 | 240.28 | 0 | 4.41 |
| ECOLL1 | 345.18 | 0 | 78.1 |
| ECOLL2 | 475.28 | 0 | 11.3 |
| TOTAL | | 60.9 | 245.8 |

## Acknowledgments

This work is supported by Department of Energy contract DE-AC02-76SF00515.

## References

[1] R. Appleby, *et al.*, SLAC–PUB–11372, presented at the LCWS 2005, Stanford, CA, USA (2005).
[2] Y. Nosochkov, *et al.*, SLAC–PUB–11363, presented at the LCWS 2005, Stanford, CA, USA (2005).
[3] Y. Nosochkov, *et al.*, SLAC–PUB–11205, presented at the PAC 2005, Knoxville, TN, USA (2005).
[4] Y. Nosochkov, *et al.*, these proceedings, http://alcpg2005.colorado.edu:8080/alcpg2005/program/accelerator/WG4/aug17_nosochkov_extraction20mrad.pdf .
[5] T. Maruyama, these proceedings, http://alcpg2005.colorado.edu:8080/alcpg2005/program/accelerator/WG4/aug17_Maruyama-backgrounds.ppt .
[6] D. Angal-Kalinin, these proceedings, http://alcpg2005.colorado.edu:8080/alcpg2005/program/accelerator/WG4/aug16_snowmass_optics_summary.ppt .
[7] B. Parker, unpublished.
[8] C. Spencer, unpublished.
[9] D. Cinabro, *et al.*, IPBI TN–2003–1 (2003).
[10] K.C. Moffeit, *et al.*, SLAC–PUB–11322, presented at the LCWS 2005, Stanford, CA, USA (2005).
[11] T. Raubenheimer, http://www-project.slac.stanford.edu/ilc/acceldev/beamparameters.html (February 28, 2005).
[12] D. Walz, these proceedings, http://alcpg2005.colorado.edu:8080/alcpg2005/program/accelerator/WG4/aug17_beam_dump_d_walz.pdf .
[13] D.C. Carey, K.L. Brown, Ch. Iselin, "Decay TURTLE," SLAC–246 (1982).